ELSEVIER

Thermochimica Acta 369 (2001) 67–78

thermochimica acta

www.elsevier.com/locate/tca

Reversibility of melting and crystallization of indium as a function of the heat conduction path☆

R. Androsch[a,*], B. Wunderlich[b]

[a]*Institute of Material Science, Martin-Luther-University, Halle-Wittenberg, Geusaer Str., 06217 Merseburg, Germany*
[b]*Department of Chemistry, The University of Tennessee Knoxville, TN 37996-1600, and Oak Ridge National Laboratory, Chemical and Analytical Sciences Division, Oak Ridge, TN 37831-6197, USA*

Received 8 June 2000; received in revised form 25 September 2000; accepted 1 October 2000

Abstract

The melting and crystallization behavior of indium has been investigated by temperature-modulated, differential scanning calorimetry as a function of thermal resistance between the heater/sensor and the sample, and as a function of the modulation parameters using a heater-controlled, heat-flux calorimeter. The thermal resistance between the heater/sensor and the indium sample was varied by placing the indium above polymer layers of different thickness. This results in apparent shifts of the onset of melting to higher temperatures and a striking reduction of the apparent degree of reversibility of melting with increasing thermal resistance. The apparent degree of reversibility is judged by an integral analysis of the modulated and total heat-flow rate, not the reversing, complex heat capacity, which is ill suited for the description of the melting process. The modulation frequency and amplitude have larger effects on the total and reversing heat-flow rate if the thermal resistance is low. A change in thermal resistance can transform a known reversible process that is coupled with a large latent heat, to an apparently non-reversing one.

Keywords: Melting; Crystallization; Indium; DSC; TMDSC; Fourier transformation; Integral analysis

1. Introduction

Temperature-modulated differential scanning calorimetry (TMDSC) has from its beginning been used to explore the reversibility of physical processes like melting and crystallization [1,2]. In general, the melt-to-crystal transition is a thermodynamically irreversible event due to the need for crystal nucleation [3–5]. If nucleation can be avoided, as for example by seeding of the melt, the phase transition may become thermodynamically truly reversible, i.e. the amorphous liquid and the crystalline phase of a one-component system co-exist in a dynamic equilibrium at constant temperature and pressure, as required by the phase rule [3]. Temperature modulation about the equilibrium melting temperature could then result in melting without superheating and crystallization without supercooling, as long as instrument lag and possible slow transformation rates are not limiting the transition. In the calorimetry of indium, a supercooling of about 1.0 K is needed for crystallization in the

☆ "The submitted manuscript has been authored by a contractor of the US Government under the contract No. DOE-AC05-96OR22725. Accordingly, the US Government retains a non-exclusive, royalty-free license to publish or reproduce the published form of this contribution, or allow others to do so, for US Government purposes".

* Corresponding author. Tel.: +49-3461-46-3762; fax: +49-3461-46-3891.
E-mail address: androsch@werkstoff.uni-halle.de (R. Androsch).

0040-6031/01/$ – see front matter
PII: S0040-6031(00)00728-0

absence of nuclei, and in their presence, reversibility was shown in modulations with amplitudes of ±0.05 K [6,7]. The crystal nucleation was avoided in the TMDSC by incomplete melting, which can result, depending on the instrument behavior [8], in completely reversing, if not truly reversible melting of indium. The term ''reversing'' is used in TMDSC for a process that displays a reversing heat-flow rate, the first harmonic of its Fourier series, as will be shown below. The term ''reversible'' is reserved for proven thermodynamic reversibility.

In the case of polymers, the irreversible character of the melting process is uniquely different. Typically a supercooling of 5–20 K is needed, even in the presence of crystal nuclei. In polymers a truly reversible melt-crystal transition can only be obtained if, in addition to crystal nucleation, molecular nucleation is not slowing the crystallization [4,9,10]. Molecular nucleation accounts for the initial step of adding a segment of a macromolecule to an existing crystal. In addition to the supercooling due to molecular nucleation, the crystal-melt transition of polymers may show superheating, either by slow melting, as observed for extended-chain crystals, or by crystals embedded in strained melts, which lower the entropy of fusion and lead to a higher melting temperature for the length of time the strain can be maintained [3,5].

A local, seemingly truly reversible melting, however, has also been observed in polymers under special conditions [11–22]. This phenomenon is not yet unequivocally explained, and seems to be restricted to the existence of a matrix of metastable crystals [22] and often does not exceed one percent per kelvin conversion, i.e. only a minor part of the total crystallinity is involved in the reversible phase transition at any one temperature. For poorly crystallized polymers and copolymers, this reversible melting stretches over a wide temperature range and may account for a sizeable fraction of the sample [20–22].

The determination of the degree of reversibility of the crystal-melt transitions is, thus, of great importance in the field of polymeric materials, and can be investigated by TMDSC. Quasi-isothermal modulation about an average temperature, T_0, i.e. modulation without an underlying heating rate $\langle q \rangle$, allows the separation of the truly reversible process from time-dependent, irreversible events. In such analyses the amplitude of the reversing heat-flow rate is made up of contributions from the true, thermodynamic specific heat capacity, and the latent heat from the transition. The latter can be described by

$$c_p^{\text{excess}} = c_p^{\text{reversing}} - c_p^{\text{thermodynamic}};$$
$$100 \times \frac{c_p^{\text{excess}}}{\Delta h_f^{100}} = \Delta h_f^{\text{reversible}} \quad (1)$$

where c_p^{excess}, $c_p^{\text{reversing}}$, and $c_p^{\text{thermodynamic}}$ are the corresponding specific heat capacities, Δh_f^{100} is a normalization factor, and $\Delta h_f^{\text{reversible}}$, the degree of reversibility in percent per kelvin and gram. In fact, Eq. (1), contains the assumption that the excess heat capacity is due to a latent-heat effect and not due to an increased thermodynamic heat capacity due to molecular motion, as is sometimes seen in the vicinity of first-order transitions, particularly those involving mesophases. This assumption is based on several independent investigations on polymers for which it was possible to identify truly reversible structural changes. The thermodynamic heat capacity which cannot be separated from the latent heat effect because of the changing phase composition at the first-order-transition temperature was, as usual, interpolated from temperatures outside of the transition. The excess, apparent heat capacity can be calculated from the heat-flow rate if steady-state is reached within the cycle of sawtooth modulation, as used in the present research

$$mc_p^{\text{reversing}} \approx \frac{\text{HF}^{\text{steady-state}}}{q} \quad (2a)$$

where m is the sample mass, and HF, the heat-flow rate. Commonly Eq. (2a) is used also for the evaluation of specific heat capacity by standard DSC [3].

To use the heat-flow rate, as it changes in sinusoidal modulation, customarily one uses the amplitude of the first harmonic, A_1, of the Fourier-transform of the heat-flow rate and the sample temperature, T_s [23,24]:

$$c_p^{\text{reversing}} = \frac{(A_1)_{\text{HF}}}{(A_1)_{T_s}\omega}\sqrt{1 + \left(\frac{C_r}{K}\right)^2 \omega^2} \quad (2b)$$

The square-root-expression was introduced as a correction term accounting for the difference between sample and reference calorimeters, with K representing the Newton's law constant, C_r, the heat capacity of the empty reference calorimeter, and ω (= 2π/period) is the fundamental frequency of the Fourier series

described below. The ratio C_r/K has the unit and physical meaning of a time constant, τ, in s rad^{-1} and can also be used to empirically account for the various heat-transfer conditions of the two calorimeters [25–27].

The heat capacity and the reversing heat capacity calculated with Eqs. (2a) and (2b), respectively, are identical as long as no slow sample response to the temperature modulation occurs, as may happen, for example, in the glass and melting transition ranges, and if the first harmonic of the Fourier series completely represents the modulated heat-flow rate, HF(t). In case of a sawtooth-modulation, which is used in this study, higher harmonics, v, are always needed for a full representation of HF(t) [25,26]:

$$\mathrm{HF}(t) = \frac{8A_{\mathrm{HF}}}{\pi^2} \sum_{1,3,5,\ldots} \left[\frac{(-1)^{(v+3)/2}}{v^2} \sin(v\omega t) \right] \qquad (3)$$

Even-numbered harmonics do not appear in Eq. (3) for a sawtooth modulation, and as long as the modulation can be made centrosymmetric there are no cosine terms as shown in Eq. (3). If Eq. (3) holds, the first harmonic is a fixed fraction of the total sum of HF(t). The specific heat capacities can then be computed from Eq. (2b), as long as both the modulation of the sample temperature and heat-flow rate are represented by the same fractions of the Fourier series. Distortions by instrument effects or irreversible thermal events cause the appearance of even harmonics and may give different fractions for the first harmonics of T_s and HF(t). For heat-flux calorimeters, linearity and symmetry of the heat-flow-rate response to temperature modulation has been proven as pre-requisite for quantitative interpretation [28–30].

In this paper, we describe an investigation of the degree of the apparent reversibility as function of the total thermal resistance between the heater/sensor and the sample of the crystal-melt transition of indium, known to be thermodynamically reversible in the presence of nuclei. The indium samples were placed at the bottom and top of layers of an inert polymer of different thickness. One piece of the indium would thus be in touch with the bottom of the calorimeter pan, the other with the lid, or open to the calorimeter atmosphere. We evaluated the influence of the average temperature gradient and the modulation amplitude within the polymer sample on the observed reversibility of the melting process of indium.

2. Experimental

The TMDSC experiments were performed with a Mettler-Toledo DSC 820 controlled at the heater, equipped with the ceramic sensor FRS 5. The instrument was operated with its liquid nitrogen accessory. The furnace and the DSC cell were purged with dry nitrogen and air, respectively, both at a flow rate of 80 ml min^{-1}. The temperature was calibrated by the onset of melting of indium and zinc, taking into account the heating rate by using the ''tau-lag calibration'' of the calorimeter. The heat-flow rate was calibrated with the heat of fusion of indium (28.45 J g^{-1}). Temperature modulation was carried out by programming the temperature to follow a symmetric sawtooth. The applied modulation amplitudes and periods were 0.025, 0.05, 0.1, 0.2, and 0.4 K and 60, 120, and 240 s, respectively. The underlying heating rate, $\langle q \rangle$ was 0.01 K min^{-1}. Indium of a mass of about 1.3 mg was placed at the bottom of the small 20 μl aluminum pan, covered with poly(butylene terephthalate) (PBT), and on top of the polymer sample, a second indium sample was placed of approximately the same mass. The thickness of the PBT sample was chosen to be either 900 or 260 μm, corresponding to polymer masses of 15.1 and 6.7 mg, respectively. The PBT melts at 493 K and, therefore, was in a partially crystalline state at the melting temperature of indium. The indium used in this study is of 99.999% purity and has a melting temperature of (429.75 ± 0.1) K. The total heat-flow rate and the reversing apparent heat capacity were calculated with the instruments software. The total heat-flow rate as average per modulation cycle is calculated directly with the Fourier-transformation-module of the software (zero Fourier coefficient), and the reversing apparent heat capacity was calculated by using Eq. (2b) with the square root correction term, set equal to one, i.e. no frequency-correction was performed.

3. Results and initial discussion

3.1. Melting by standard DSC

Fig. 1 shows standard DSC heating scans of two different samples, one covered and the other not covered with an aluminum lid. The bottom curve

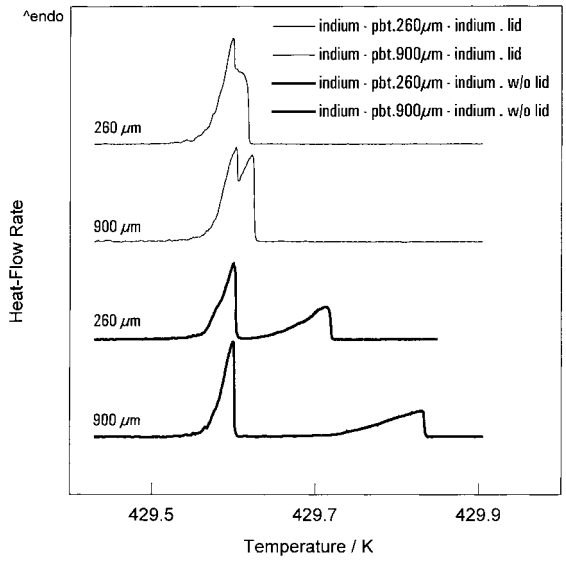

Fig. 1. Melting of indium by standard DSC at 0.01 K min^{-1} with different experimental setups, as indicated in the figure.

shows the melting peaks of the two indium samples separated by a polymer layer of 900 μm thickness, and not covered by the aluminum lid of the sample pan. The next bold-line curve shows the melting of two indium samples separated by a polymer layer of only 260 μm thickness, also not covered by a lid. The upper two curves were taken using the same sample arrangements, but covered tightly by an aluminum lid. The heating rate was 0.01 K min^{-1}, the same rate which is also used in the following TMDSC-experiments as the underlying heating rate, $\langle q \rangle$. The low-temperature melting-peak corresponds to the sample at the bottom of the pan and is unaffected by the thermal resistance of the polymer. The high-temperature-melting-peak in each of the four curves is caused by the sample on top of the polymer. Since indium is known from quasi-isothermal experiments to melt within 0.1 K or less [7,8], all deviations from sharp, reversible melting must be caused by the heat-conduction path, instrument-lag, and limits of the deconvolution of the reversing signal [14].

The onset of the melting temperature of indium and the shape of the peak depend strongly on the thickness of the polymer and on being covered by an aluminum lid or not. When not covered by a lid, the onset of the melting temperature of the indium sample at the top undergoes an apparent shift of the melting temperature by about 0.2 or 0.1 K for the 900 and 260 μm polymers, respectively. Furthermore, the slopes of the melting peaks on the low-temperature side decrease with increasing thickness of the polymer layer, and are much shallower than those of the indium samples at the bottom of the pan. The latter are indirectly proportional to the thermal resistances between heater and sample [31]. In case the sample is covered by an aluminum lid, the melting process of the indium sample at the top of the polymer is shifted much less (<0.05 K), but is still separated from the melting process at the bottom. It is obvious that the heat flow into the top-indium sample follows preferentially along the aluminum path via the lid, and not through the polymer layer. This result underscores the importance of a tight connection between sample and lid, and verifies the experimental results about temperature gradients in TMDSC obtained by infrared thermography [32].

3.2. Melting by TMDSC

Fig. 2a is a plot of the modulated (thin line) and total (bold line) heat-flow rates as a function of time, measured by TMDSC on the sample which is represented by the bottom curve in the standard DSC data of Fig. 1. Fig. 2b–d show for the same sample arrangement an enlargement of the total heat-flow rates (Fig. 2b), the reversing apparent specific heat capacities (Fig. 2c) as calculated from Eq. (2b), and the integrations of the total heat-flow rates in terms of conversion of indium to the melt (Fig. 2d) as proposed in [14]. All curves are plotted as functions of the reference temperature and are given for different modulation amplitudes. The influence of the modulation amplitude and period on the apparent reversing heat capacity during melting of the top-indium sample is shown in Fig. 3 with an expanded scale compared to Fig. 2c. Fig. 4a–d are equivalent to Fig. 2a–d, but with the two indium samples separated by the thinner PBT-layer of 260 μm and covered by an aluminum lid.

As expected from the standard DSC experiments of Fig. 1, the modulated heat-flow rates in Fig. 2a reveal two clearly separated melting processes. The first melting peak is characterized by a strong increase of the heat-flow-rate amplitudes, whereas the second melting process does not develop an increase in the amplitudes. The total heat-flow rate from the TMDSC

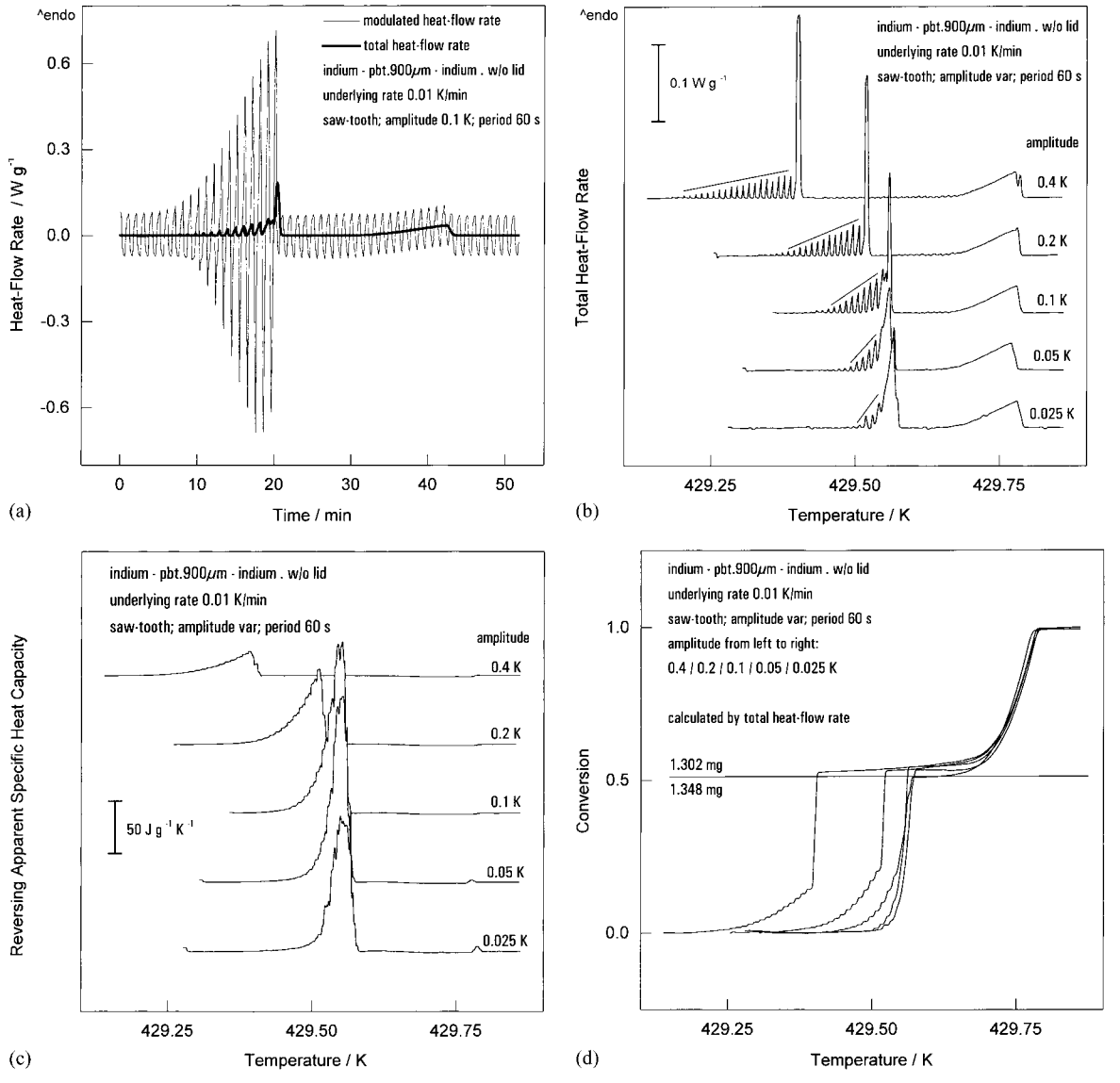

Fig. 2. (a) Modulated (thin line) and total (bold line) heat-flow rates as function of time by TMDSC, obtained simultaneously on two indium samples separated by a layer of 900 μm PBT, not covered by an aluminum lid. The modulation amplitude and period are 0.1 K and 60 s, respectively, and the underlying heating rate is 0.01 K min^{-1}. (b) The total heat-flow rate as function of reference temperature at different modulation amplitudes, sample as in Fig. 2a. (c) Reversing apparent specific heat capacity as function of reference temperature at different modulation amplitudes, sample as in Fig. 2a. (d) Conversion of indium to the melt as a function of reference temperature at different modulation amplitudes calculated from data shown in Fig. 2b. The mass of the bottom and top samples are 1.348 and 1.302 mg, respectively, and the horizontal line slightly above a conversion of 0.5 marks the expected total conversion of the bottom sample.

associated with these two melting events is also different and corresponds to the standard DSC experiment of Fig. 1 only in area, not in shape. The first melting event has periodic subsidiary peaks before the final melting which result in an increasing nonreversing component on deconvolution of the melting process. The second melting event, which is assigned to the indium sample on top of the 900 μm-polymer layer, occurs over a much larger temperature interval. The total heat-flow rate appears smooth and almost all

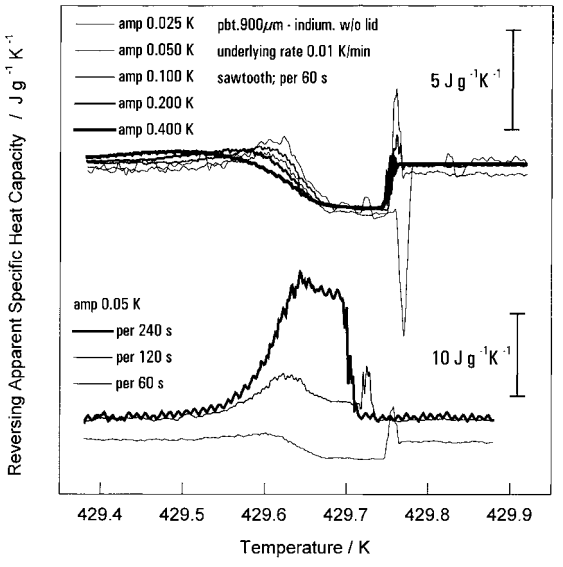

Fig. 3. Reversing apparent specific heat capacity in the melting region of the top indium sample as function of temperature at different modulation amplitudes, and as function of different modulation periods. The pan contained a 900 µm thick layer of PBT, and only a top sample of indium. The other conditions are as in Fig. 2.

melting appears in the nonreversing component. Quite clearly the increased instrument lag due to the intervening polymer layer supplants the inherent reversibility of the melting of indium.

3.3. Influence of the modulation amplitude on the melting of the bottom indium sample

The modulation amplitude strongly affects the melting process of the bottom-indium sample, but causes little changes for the melting process of the indium sample at the top (Fig. 2b–d). An increasing modulation amplitude shifts the onset and end of the apparent melting process to a lower temperature and the apparent reversing heat capacity has a lower maximum and area. These observations are also mirrored in the integral plot of Fig. 2d, which represents the normalized crystal-to-melt conversion versus temperature, obtained by integration of the total heat-flow rate of Fig. 2b.

The dependence of the beginning of melting on the modulation amplitude can be explained on the basis of Fig. 5. The average temperature of first melting when using modulation with an underlying heating rate must depend on the modulation amplitude, since for higher amplitudes the first melting can occur at lower average temperatures. The true melting point of a sample, which is represented by the abscissa in Fig. 5, is reached at a lower average modulation temperature (open squares) if the amplitude is increased. This can also be evaluated by the lag of the sample temperature behind the reference temperature. As soon as melting starts, the sample temperature remains largely constant, and lags behind the reference temperature. On standard DSC, the first deviation of the sample temperature due to melting is at 429.53 K, i.e. first melting by TMDSC is observed at the average temperature $(429.53 - A_{T_s})$ K.

The TMDSC melting processes can be understood by assessing the effect on the sample temperature. Fig. 6 shows the final melting range of the bottom sample, using the last four modulation cycles before completion of melting. Melting is indicated by the lag of the sample temperature (■) relative to the program temperature (or reference temperature), marked by the thin line. Crystallization, analogously, is signified by the larger sample temperature (■) relative to the program temperature. Except for the last cycle, melting is incomplete, as indicated by the straight-line change-over from melting to crystallization. In case of modulation with an amplitude of 0.05 K (lower graph), a large fraction of the indium melts in each cycle and the subsequent crystallization is incomplete, so that the programmed temperature is only reached after complete melting in the last cycle. After all crystals are melted, no nuclei for the subsequent crystallization remain, and the decrease of temperature is not sufficient to overcome the needed supercooling for nucleation. In the case of the modulation amplitude of 0.4 K (upper graph), in contrast, after the lesser amount of melting in the shorter time above the melting temperature, the crystallization is almost complete and the programmed temperature is approached. Note that for both experiments melting continues beyond the peak in the sample temperature, as seen in the last cycles of melting where no subsequent crystallization occurs.

The lag between sample and reference temperatures during crystallization also reveals the nonreversing components which accumulate in the averages over one modulation cycle versus the average temperature

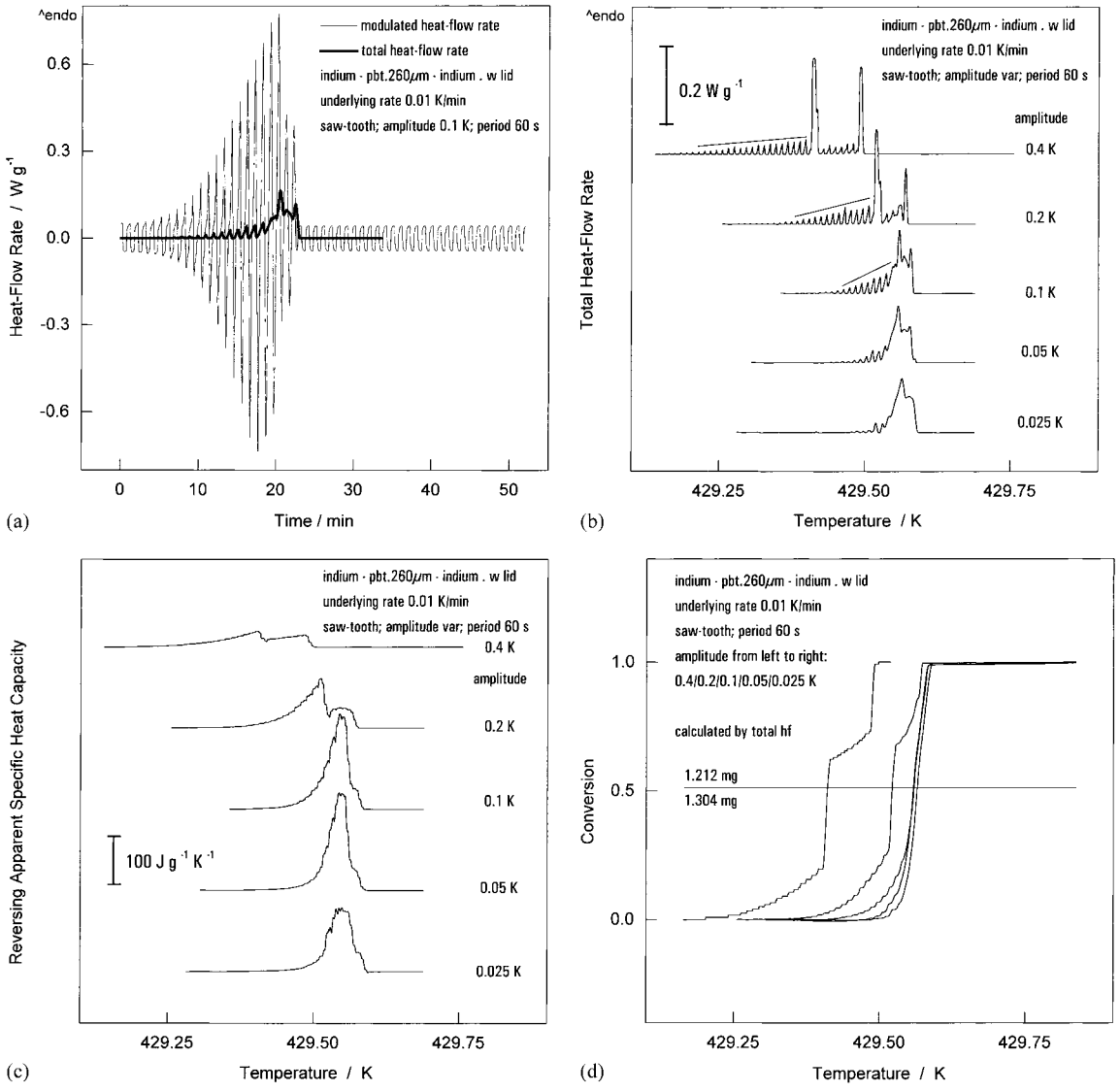

Fig. 4. (a) Modulated (thin line) and total heat-flow rate (bold line) as function of time, obtained simultaneously on two indium samples separated by a layer of 260 μm PBT, covered by an aluminum lid. The modulation amplitude and period are 0.1 K and 60 s, respectively, and the underlying heating rate is 0.01 K min^{-1}. (b) Total heat-flow rate as function of reference temperature at different modulation amplitudes, sample as in Fig. 4a. (c) Reversing apparent specific heat capacity as function of reference temperature at different modulation amplitudes, sample as in Fig. 4a. (d) Conversion of indium to the melt as a function of reference temperature at different modulation amplitudes calculated from data shown in Fig. 4b. The mass of the bottom and top samples are 1.304 and 1.212 mg, respectively, and the horizontal line slightly above a conversion of 0.5 marks the expected total conversion of the bottom sample.

and accounts for the small peaks in the total heat-flow rate (Fig. 2b) and the steps in the cumulative integral (Fig. 2d), as first shown and modeled in [14]. These steps are not a sign of irreversible melting, but the result of instrument lag and failure of the first harmonic to properly account for heat flows that are not constant, sinusoidal with frequency ω, or change linearly with time. Indium, known to melt reversibly in presence of nuclei, changes in apparent reversibility with modulation amplitude (see also Fig. 7 in [8]). The

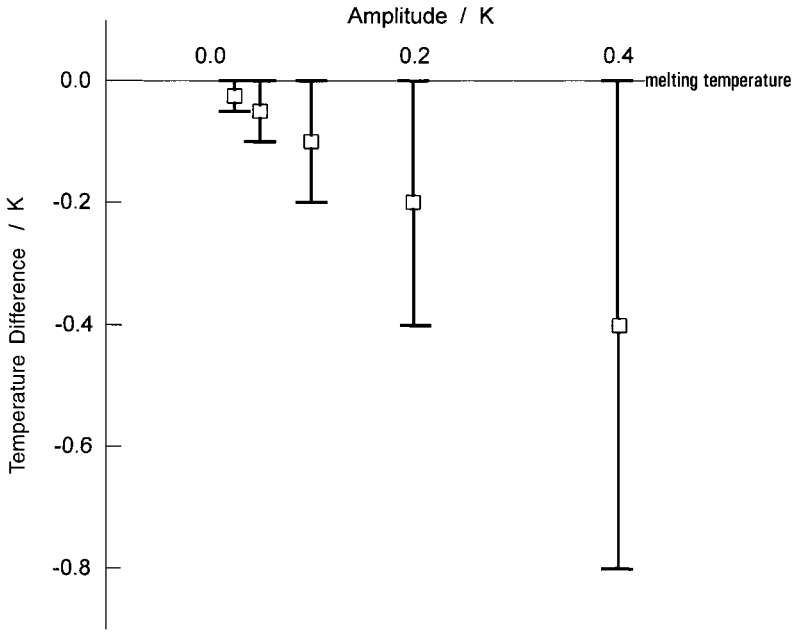

Fig. 5. Schematic of the shift of the average modulation temperature (open squares) of first detection of melting with variation of the modulation amplitude. The abscissa is considered to be the melting temperature and the bars represent the heating and cooling branch of the modulation about the average temperature which is given by the open squares.

modulation amplitude controls the available time for melting at a constant, instrument-controlled rate: the larger the modulation amplitude and the closer the melting point is to the minimum modulation temperature, the more time is available for melting within one modulation cycle. The apparent reversing heat capacity during the melting of indium seen in Fig. 2c, often taken as the benchmark to judge reversibility of a physical or chemical process, decreases with modulation amplitude and obviously does not permit to draw any conclusions about the true degree of reversibility. The apparent reversing heat capacity is sensitive to the absolute latent heat which is exchanged during modulation (see the step size in Fig. 2d), but obviously it cannot give information about the true reversibility of a transition.

Fig. 2d, furthermore, shows that the amount of apparently irreversibly melting material per modulation cycle increases with decreasing amplitude which, again, is explained by the asymmetry between melting and subsequent crystallization. The heat of fusion within the final melting step also depends on the modulation amplitude. It is set by the amount of crystals in the last melting step (residual crystals from the next-to-last melting and newly crystallized crystals). The onset temperatures of the melting process are lowered exactly with the modulation amplitude, however, the temperature differences are less when melting is finished, because of the asymmetry introduced in the modulation by the absence of nuclei as soon as all indium is melted.

For different experimental setups, i.e. by using a different polymer thickness or changing the covering option for the pan, the melting of the bottom-indium sample shows no change in its onset of melting, as documented in Fig. 4b–d, its reversing apparent heats of transition, as seen in Fig. 4c, and its temperature of completion of melting, as observed in Fig. 4b–d.

3.4. Influence of the modulation amplitude on the melting of the top indium sample

The trends observed for the melting process of the indium sample placed on top of the polymer layer are different from the indium at the bottom. In Fig. 2b, the total heat-flow rates practically show no changes of the onset temperature or width of the melting process with modulation amplitude. The melting peak is almost

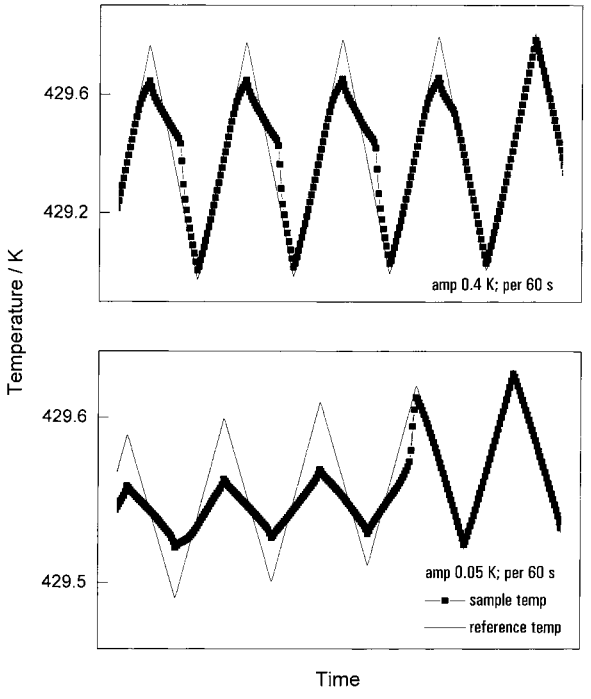

Fig. 6. Programmed temperatures (thin line) and sample temperatures (squares) as function of time during melting of indium at the bottom of the pan, using the same sample as in Fig. 2. The modulation amplitudes are 0.4 K (top) and 0.05 K (bottom), the modulation period is 60 s and the underlying heating rate, 0.01 K min^{-1}.

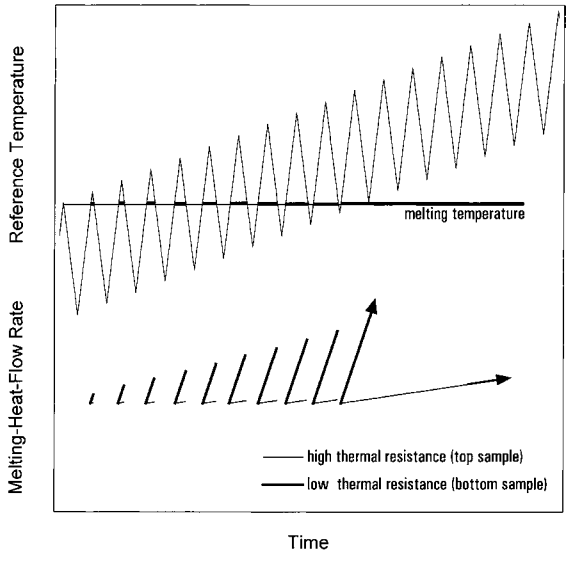

Fig. 7. Schematic of the heat-flow rate, caused by melting of samples with high and low thermal resistance between sample and heater/sensor, corresponding to the top and bottom indium samples, respectively. The upper curve is the sawtooth-modulated reference temperature with a non-zero underlying heating rate. The horizontal line is the virtual melting temperature where the thick-drawn parts indicate possible melting since the reference temperature is above the melting temperature. The lower part shows schematically the heat-flow rate for samples of high (thin line) and low thermal resistance (thick line) as one would observe in the regions where the reference temperature is higher than the melting temperature. Final melting occurs at the latest if the reference temperature stays above the melting temperature with its minimum temperature (indicated by the arrows, or last segment of the melting-heat-flow rate, respectively).

unchanged compared to that of Fig. 1 (bottom curve). The modulated heat-flow rate in Fig. 2a indicates that over the broad melting range the latent heat is practically not modulated, i.e. it contributes almost nothing to the apparent reversing heat capacity of the melting in Fig. 2c.

To verify the results on the indium sample on top of the polymer without lid, we have repeated the measurements with runs which contained only an indium sample at the top of 900 μm thick polymer. The apparent, reversing heat capacity of this experiment is plotted with an enlarged scale in Fig. 3. As can be seen, in particular for the measurement with a low modulation amplitude (0.025 K), the apparent reversing heat capacity slightly increases above the value which is caused by the total apparent heat capacity outside of the transition (due to the heat capacity of indium + PBT + a possible asymmetry correction). This small increase is followed by a more abrupt decrease, and finally recovery of its initial value after completion of the transition. Albeit all effects are very minor compared to the total melting peak of the bottom-indium sample, the earlier discussed trends of the onset temperature of the process and the maximum and area of the initial increase of the apparent reversing heat capacity can also be observed for this sample.

The decrease of the apparent reversing heat capacity below the level of the true heat capacity contribution in Eq. (1) for modulation periods of 60 s is surprising. It is caused by a different partition of HF(t) and $T_s(t)$ among the first and higher harmonics (nonlinearity of heat-flow-rate response). A much stronger deviation of the measured sample temperature from the programmed temperature is seen in Fig. 6 for the bottom sample of

indium. In this case, however, the amplitude of the heat-flow rate is sufficiently increased due to the additional melting and crystallization to not show a decrease in the apparent reversing heat capacity of Fig. 2c. The sharp peaks at the end of melting in Fig. 3 are also artifacts in the first harmonic of the Fourier series and change with the relative phase shift of the cessation of the latent heat effects [33].

The cumulative integral of the total heat-flow rate (Fig. 2d) documents the difference of the melting behavior of indium at the bottom of the pan and at the top of the polymer. The melting process of the top sample occurs almost unaffected by the modulation, but broadened and shifted to higher temperature, similar to the standard DSC.

The data of Fig. 4d, of indium samples separated by 260 μm of PBT and covered by an aluminum lid, reveal that the melting of the two indium samples overlap, but are similar in nature. After the melting of the bottom-indium is finished, the total heat of fusion jumps to a value larger than expected, i.e. to a value higher than 50%. Obviously, the top-indium sample starts melting before melting of the bottom sample is completed. As expected from the data of Fig. 1, the melting of the top indium is increasingly affected by the modulation in the following order of the experimental setup: [indium-PBT.260 μm-indium; covered] > [indium-PBT.900 μm-indium; covered] > [indium-PBT.260 μm-indium; uncovered] > [indium-PBT.900 μm-indium; uncovered].

3.5. Influence of the modulation period on the melting of the top indium sample

Additional, not shown, experiments with higher modulation periods lead to similar observations of larger modulation of the melting of indium at the bottom of the polymer, whereas the top indium is barely modulated. The onset temperatures of melting of the bottom and top indium and the total heat-flow rates are almost unchanged when the frequency is varied. The apparent reversing heat of fusion of the melting process systematically increases with decreasing frequency. On melting of the top-indium sample, a similar trend of a decrease of the heat-flow-rate amplitude after an initial increase is observed in Fig. 3, but for periods less than 60 s they remain higher than the melt values.

Inspection, for instance, of the cumulative integrated heat of fusion reveals that the decrease of the apparent reversing heat capacity within the melting range is caused by the largely nonreversing characteristics of the melting process produced by the experimental setup. By its lags it causes continuing melting, even within the programmed cooling branch, and the different apparent rates of melting during heating and (melting + crystallization) during cooling control the magnitude of the apparent reversing heat capacity.

As shown in infrared thermography of the various positions within the DSC cell [32], the modulation amplitude decreases as function of the position x within the sample proportionally to $\exp[-x(\pi/(k \times \text{period}))^{1/2}]$, where k is the thermal diffusivity. An increased modulation period, therefore, results in a less damped modulation amplitude at the top of the sample, and is responsible for the increase of the reversing apparent heat capacity in its maximum value/integral.

4. Final discussion and conclusions

The scope of the investigation was to explore the effect of the heat transfer condition on the total and reversing components of the heat-flow rate during a first order crystal-melt transition that is known to be practically reversible in the presence of crystal nuclei. The heat capacity when determined by standard DSC with Eq. (2a), naturally, applies to the average temperature with respect to the distribution throughout the entire sample, an error which is relatively small because of the small change of heat capacity with temperature. For TMDSC, in contrast, the reversing heat capacity according to Eq. (2b) is taken to be proportional to the heat-flow rate amplitude divided by the measured sample temperature amplitude. If, however, the modulation amplitude at the top of the sample decreases with the thickness of the sample, the heat capacity is in error proportionally to this decrease in amplitude, i.e. the effect is much larger and needs extensive corrections. This error caused by the thickness of the sample when only measuring the thermodynamic heat capacity by TMDSC has been studied recently [25]. It could be corrected by a sample-specific function determined from the

frequency-dependence of the uncorrected apparent heat capacity [25–27]. Adding an equilibrium first-order transition in a one-component system it must be assumed that the transition occurs at constant temperature and pressure when crystal nuclei are present. The temperature gradients within such samples are then more complicated. As soon as melting begins, the interfaces between crystal and melt remain at constant temperature until melting is completed. On oscillating about the melting temperature, this interface between crystal and melt will recede and advance as the temperature is modulated. Inside the remaining crystal, the temperature gradient will quickly diminish and settle at the melting temperature. The melt outside of the remaining crystal, however, can attempt to follow the temperature modulation. Only after melting is complete, will the prior temperature gradient be reestablished, altered as required by the changed thermal diffusivity[1]. The heat-flux calorimeter used in this research employs a single flat heater underneath sample and reference so that as a first approximation, an axial temperature gradient develops from the bottom to the top of the sample. On heating and cooling, the average temperature at the bottom of the sample will be at a higher, respectively, lower temperature than the top of the sample. The lag between bottom and top of the sample depends on the thermal diffusivity of the sample, its thickness, and the heating rate. The data of Fig. 1 reveal that the lag is about 0.2 K at a heating rate of 0.01 K min^{-1} for a typical polymer sample of almost 1 mm thickness. In TMDSC, this lag of 0.2 K would be related to the underlying heating rate, and furthermore the modulation amplitude and phase angle relative to the change of reference and sample temperature relative to the axial position within the sample.

Summarizing, there are at least three effects which explain the different melting behavior of the bottom and top indium sample: (A) the underlying temperature gradient from bottom to top within the sample pan; (B) the gradient of the modulation amplitude and the phase lag; and (C) the changing thermal resistance from bottom to top. With respect to the melting process, effects (A) and (B) will cause a smearing of the heat-flow rate signal versus temperature (see for instance Fig. 1), and effects (B) and (C) will result in modified apparent heat-flow rates, and change the apparent degree of reversibility of the melting process. The magnitude of effects (A) and (B) are derived in standard textbooks [34]. They were recalculated for specific TMDSC-conditions [35,36] and experimentally verified [32].

The decrease of the apparent rate of melting and the decreased degree of reversibility of the melting process with increasing thermal resistance can qualitatively be visualized by the schematic in Fig. 7, which is not based on any simulation or calculation. The upper sawtooth is the reference or program temperature. The horizontal bold line segments mark the times when the reference temperature is above the melting temperature. With ongoing time, these sections are getting increasingly longer because of the underlying heating rate. Only within these sections melting can occur, with its rate controlled by the thermal resistance of the system. The heat-flow rates caused by melting are shown by the lower two curves for high (thin line) and low (thick line) resistances, as experienced at the top of the polymer and the bottom of the sample pan. The order of magnitude of the heat-flow rates due to melting can be gained from Fig. 1. The crystallization occurs in the intermediate times and is not shown since it is not controlled by the heat-transfer condition from the heater, but rather by the absolute temperature. In case the apparent rate of melting is high (thick line), the melting process will be much faster. It may perhaps complete melting before the minimum temperature of the modulation reaches the melting temperature. The reversing melting stops when in one cycle melting completes, since the cooling cycle can then not reach the supercooling needed to nucleate and grow crystals again. In case the apparent rate of melting is low (thin line), the melting process might be extended beyond the time when the minimum temperature in the oscillation exceeds the melting temperature. The decreased modulation amplitude at the top of the sample, compared to the amplitude at the bottom, enhances the above described effect considerably (see Fig. 6) and the apparent nonreversing character of the transition is increased.

The experiments on indium have shown that the reversing apparent heat capacity in the crystal-to-melt transition is controlled by instrumental parameters including the heat transfer between heater, sensor,

[1] The thermal diffusivity is the thermal conductivity divided by the specific heat capacity and the density.

and sample, as well as the parameters of modulation and the deconvolution techniques used for the data analysis. In case of a reversible transition, like the melting of indium in the presence of nuclei, the process can appear as fully reversing or nonreversing or as any intermediate case. If the transition is not as narrow as for indium, the transition must be treated as a superposition of separate events. Qualitative and quantitative analysis of the reversibility of transitions by TMDSC is limited by the maximum heat-flow rate, the constancy of the temperature of the crystal during melting, the crystallization kinetics on cooling, the possibly missing nucleation, the change of the average temperature of modulation, and the increasing thermal resistance with sample thickness which causes an apparent reversibility spectrum if the samples are of low thermal conductivity, as is usual for polymers. Thin samples and long-time quasi-isothermal analyses are the tools developed to avoid these problems.

Acknowledgements

This work was supported by the Division of Materials Research, National Science Foundation, Polymers Program, Grant No. DMR-9703692 and the Division of Materials Sciences and Engineering, Office of Basic Energy Sciences, US Department of Energy at Oak Ridge National Laboratory, managed and operated by UT-Batelle, LLC, for the US Department of Energy, under contract No. DOE-AC05-00OR22725.

References

[1] P.S. Gill, S.R. Sauerbrunn, M. Reading, J. Therm. Anal. 40 (1993) 931.
[2] M. Reading, D. Elliot, V.L. Hill, J. Therm. Anal. 40 (1993) 949.
[3] B. Wunderlich, Thermal Analysis, Academic Press, New York, 1990; updated as Thermal Analysis of Materials. A computer-assisted lecture course of 36 lectures and 2879 screens, published on the Internet (web.utk.edu/~athas/courses/tham99.html), downloadable including presentation software, 2000.
[4] B. Wunderlich, Macromolecular Physics, Vol. 2, Crystal Nucleation, Growth, Annealing, Academic Press, New York, 1976.
[5] B. Wunderlich, Macromolecular Physics, Vol. 3, Crystal Melting, Academic Press, New York, 1980.
[6] A. Boller, M. Ribeiro, B. Wunderlich, J. Therm. Anal. 54 (1998) 545.
[7] K. Ishikiriyama, A. Boller, B. Wunderlich, J. Therm. Anal. 50 (1997) 547.
[8] R. Androsch, B. Wunderlich, Thermochim. Acta, in press.
[9] B. Wunderlich, Disc. Farad. Soc. 68 (1979) 239.
[10] S.Z. Cheng, B. Wunderlich, J. Polym. Sci., Part B: Polym. Phys. 24 (1986) 595.
[11] Y. Tanabe, G.R. Strobl, E.W. Fischer, Polymer 27 (1986) 1147.
[12] G.R. Strobl, M.J. Schneider, G. Voigt-Martin, J. Polym. Sci., Polym. Phys. 18 (1980) 1361.
[13] J.M. Schultz, E.W. Fischer, O. Schaumburg, H.A. Zachmann, J. Polym. Sci., Polym. Phys. 18 (1980) 239.
[14] B. Wunderlich, A. Boller, I. Okazaki, K. Ishikiriyama, W. Chen, M. Pyda, J. Pak, I. Moon, R. Androsch, Thermochim. Acta 330 (1999) 21.
[15] I. Okazaki, B. Wunderlich, Macromolecules 30 (1997) 1758.
[16] K. Ishikiriyama, B. Wunderlich, Macromolecules 30 (1997) 4126.
[17] C. Schick, M. Merzlyakov, B. Wunderlich, Polym. Bull. 40 (1998) 297.
[18] A. Wurm, M. Merzlyakov, C. Schick, J. Therm. Anal. 56 (1999) 1155.
[19] A. Wurm, M. Merzlyakov, C. Schick, Coll. Polym. Sci. 276 (1998) 289.
[20] R. Androsch, Polymer 40 (1999) 2805.
[21] R. Androsch, B. Wunderlich, Macromolecules 32 (1999) 7238.
[22] R. Androsch, B. Wunderlich, Macromolecules, 2000, accepted.
[23] B. Wunderlich, Y. Jin, A. Boller, Thermochim. Acta 238 (1994) 277.
[24] A. Boller, Y. Jin, B. Wunderlich, J. Therm. Anal. 42 (1994) 307.
[25] R. Androsch, I. Moon, S. Kreitmeier, B. Wunderlich, Thermochim. Acta 357/358 (2000) 267.
[26] R. Androsch, B. Wunderlich, Thermochim. Acta 333 (1999) 27.
[27] R. Androsch, J. Therm. Anal. Calor. 61 (2000) 75.
[28] T. Ozawa, K. Kanari, Thermochim. Acta 253 (1995) 183.
[29] M. Merzlyakov, C. Schick, Thermochim. Acta 330 (1999) 55.
[30] J.E.K. Schawe, E. Bergmann, W. Winter, J. Therm. Anal. 54 (1998) 565.
[31] W.F. Hemminger, H.K. Cammenga, Methoden der Thermischen Analyse, Springer, Berlin, 1989.
[32] R. Androsch, M. Pyda, H. Wang, B. Wunderlich, J. Therm. Anal. Calor. 61 (3) (2000) 661.
[33] M.L. Di Lorenzo, B. Wunderlich, J. Therm. Anal. Calor. 57 (1999) 459.
[34] H. Gröbers, S. Erk, Fundamentals of Heat Transfer, McGraw-Hill, New York, 1961.
[35] F.U. Buehler, C.J. Martin, J.C. Seferis, in: K.R. Williams, (Ed.), Proceedings of the 26th NATAS Conference, Cleveland, OH, 13–15 September 1998, Vol. 26, p. 44.
[36] F.U. Buehler, J.C. Seferis, J. Therm. Anal. 54 (1998) 1.